Compact hybrid real-time hyperspectral imaging system with high effective spatial, spectral, and temporal resolution

Conference Paper · October 2016

DOI: 10.1117/12.2246110

CITATIONS
0

READS
268

5 authors, including:

Filip Roth
Masaryk University
4 PUBLICATIONS **2** CITATIONS
SEE PROFILE

Ahmad Abbadi
Masaryk University
13 PUBLICATIONS **47** CITATIONS
SEE PROFILE

Ondřej Herman
Masaryk University
11 PUBLICATIONS **9** CITATIONS
SEE PROFILE

Vaclav Prenosil
Masaryk University
61 PUBLICATIONS **557** CITATIONS
SEE PROFILE

Compact hybrid real-time hyperspectral imaging system with high effective spatial, spectral, and temporal resolution

Filip Roth*[a], Ahmad Abbadi[a], Ondrej Herman[a], Martin Pavelek[a], Vaclav Prenosil[a]
[a]Faculty of Informatics, Masaryk University, Botanicka 68a, Brno, Czech Republic

ABSTRACT

Medical endoscopes for image-guided surgery commonly use standard color image sensors, discarding any more detailed spectral information. Medical spectroscopy devices with various spectral working ranges are specialized to specific medical procedures and in general are not usable for image-guided surgery due to limitations in spatial or temporal resolution.

In this paper, we present an initial demonstrator of hyperspectral endoscope, composed of two image sensors with complementing parameters. Using this hybrid approach, combining sensors with different spatial and spectral resolutions and spectral ranges, we obtain improved coverage of all the respective parameters. After digitally processing and merging the video streams, while maintaining the better features of both, we obtain an imaging system providing high effective spatial, spectral, and temporal resolution.

The system is based on field programmable gate arrays. It provides real-time video output (60 Hz), which is usable for navigation during image-guided surgery. The flexible system architecture allows for an easy extension of the processing algorithms and enables minimal video signal latency.

Physical dimensions and portability of the system are comparable to standard off-the-shelf medical endoscope cameras. The device can output both processed video and standard visible light video signals on one or more video outputs of the system. The resulting processed video signal obtained from the combined image sensor data greatly increases the amount of useful information available to the end user.

Keywords: real-time imaging system, spatial-spectral resolution, hyperspectral endoscope, video rate processing, medical spectroscopy, image-guided surgery

1. INTRODUCTION

Medical spectroscopy is a viable approach for obtaining specific properties of biological tissues, not otherwise available for evaluation. Traditionally, medical spectroscopy has been more of an off-line method, where the biological samples are analyzed in dedicated labs outside of the operating rooms. Spectroscopy devices are in general not used during surgeries, particularly due to the fact that the image acquisition and evaluation take too long to be useful in real time. The application potential of medical spectroscopy to the invasive or minimally invasive laparoscopic procedures is significant and mandates further research into this area.

Hyperspectral imaging (HSI) is emerging as a promising imaging modality for medical applications. It works by dividing the electromagnetic radiation spectrum into many separate wavelength ranges using spectral filters of various constructions. HSI goes beyond the standard red, green and blue (RGB) three band visible light image to a more informative approach by capturing the reflectance of the material, which is sampled in tens or hundreds of spectral bands of visible or invisible electromagnetic radiation. Since each material has a unique spectral profile, knowing these profiles helps to improve region classification based on the constituent material spectra.

HSI systems generate high dimensionality images, which can be seen as a set of individual wavelength-dependent images, as shown in Fig. 1. With RGB images, the picture data is composed of three planes corresponding to the red, green, and blue channels, while with the hyperspectral imagery, the number of channels (bands) grows to ten or more depending on the physical system used for data acquisition.

*filip.roth@mail.muni.cz; www.fi.muni.cz

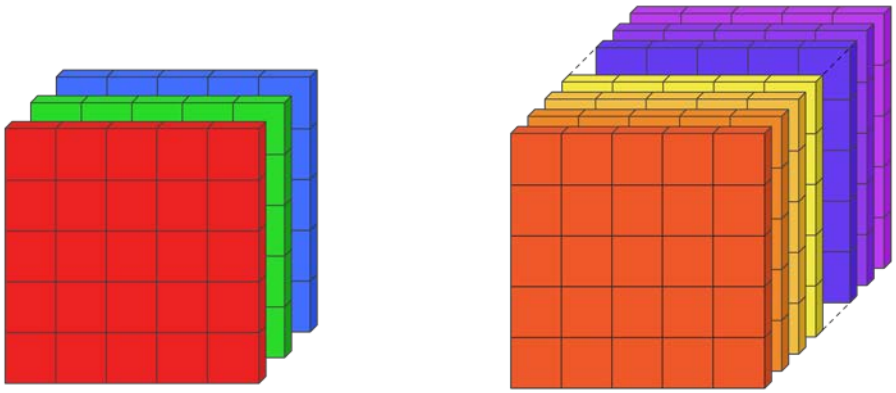

Figure 1. RGB image composed of three channels (left) compared to a hyperspectral image containing significantly more bands (right).

Many methods have been proposed for the acquisition of a hyperspectral image, each using a specific principle of operation. Some of the methods scan the image array pixel by pixel and acquire the complete spectrum for every pixel, the same idea applied in other approaches scans the field line by line[1]. The methods differ in scanning modes, whether the spectral bands are sampled in different times or whether for each pixel or line the entire spectral profile is obtained. These approaches use different physical techniques for measuring a desired spectral band response, be it optical prisms or gratings, wavelength filters, time-based analytical methods, etc.

Dispersive methods using optical prisms or diffraction gratings can be thought of as a single spectral pixel being measured at a single given time. The spatial location of the image to be scanned must be pre-selected using a suitable optomechanical apparatus. Although having a high spectral resolution, scanning an entire image using this method is relatively slow and therefore the temporal resolution is not usable for video applications[2]. Fourier transform infrared (FTIR) is a similar technique in this regard, since it again measures only a single given pixel at a time.

Bandpass optical filters can be used in systems which sample an entire region of interest (ROI) for a given band at a single time. The filters can be either exchanged mechanically[2] or controlled in a different way to select a desired spectral range. Examples of basic working principles of this class of imaging systems are liquid crystal tunable filters (LCTF) controlled by an electronic signal or acousto-optical tunable filters (AOTF) controlled by sound waves. Systems based on bandpass filters sample the image one band at a time, with non-trivial filter reconfiguration and band sampling times. Therefore, the temporal resolutions are rather low and decrease with the number of sampled spectral bands.

In recent years, a new class of spectral image sensors became available in sample quantities[3]. The sensors are based on standard CMOS image sensor manufacturing technology, which is complemented by an additional layer of bandpass filters atop of each physical sensor pixel. In principle, the filters are based on the Fabry-Perrot interferometer (etalon) with the resonance frequency tuned to the individual wavelengths desired to be sampled[3]. Since this type of spectral image sensor is based on a standard image sensor technology, the temporal resolution of this class of sensor can be very high and compatible with video or machine vision applications. For an example pixel layout of the sensor, please see Fig. 2 below.

Figure 2. An illustration of the layout of spectral filters in the hyperspectral image sensor. The mask is similar in principle to the classic Bayer pattern mask.

However, the limitation of etalon based image sensors is the spatial resolution. A standard image sensor has a mosaic of (usually) red, green and blue filters atop of each physical pixel arranged in a variation of Bayer color mask pattern[4]. This mask is most often repeated in a square 2 × 2 pixels grid. This per-pixel color filtering limits the effective spatial resolution of the sensor, since a single physical pixel senses only one of the three primary colors at its location. This disadvantage is further increased with the etalon-based spectral sensors having significantly more spectral bands. Such sensor, using for example 25 spectral bands, requires the very same 25 physical chip pixels for a single hyperspectral pixel. Therefore, instead of the 2 × 2 pixel grid pattern, the etalon-based spectral sensor requires a 5 × 5 physical pixel grid for each hyperspectral pixel (as illustrated in Fig. 3). Compared to e.g. a monochrome image sensors, this results in significantly lower spatial resolution, although with high frame rate.

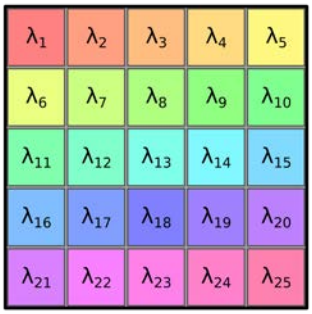

Figure 3. Detail of a single hyperspectral cell composed of 25 physical sensor pixels.

The simple solution therefore is to use two image sensors with different spatio-spectral parameters to overcome the limitations of the individual sensors and to enhance the effective quality of the resulting processed image[5]. There are certainly many ways of combining separate image sensor data into one user output, but with the intended medical

application, some of them are more advantageous. This paper describes an imaging system based on the dual sensor approach.

Having two image sensors means there are the two spectral sensitivity ranges as well, one for each sensor. There certainly are applications where the spectral ranges could overlap, but for the intended medical use case the spectral ranges were selected to be (largely) non-overlapping.

An interesting, yet relatively easy to sample with standard optical components, is the spectral region of near-infrared (NIR) electromagnetic radiation (example in Fig. 4). This wavelength range is located next to the standard visible light region, from approximately 700 nm to about 1400 nm, and in the lower wavelength part can be (with varying levels of success) imaged with optical components originally optimized for the visible light region. Although not part of the core optical path of the proposed system, the optical coatings of the peripheral (endoscopic) components are so far not optimized for the extended wavelength range, however, this did not affect the operation of the initial demonstrator system in a major way.

From the medical standpoint, there are many interesting parameters of biological tissues, which can be sampled, digitally processed, and displayed to the end user of the proposed system. The literature contains many examples of physiological properties detectable within this spectral region[6-9]. Some key parameters are blood oxygenation levels or NIR fluorescence imaging markers. Due to the higher penetration depths of electromagnetic radiation within this region, shallow vein subsurface imaging might also be a viable modality for the system.

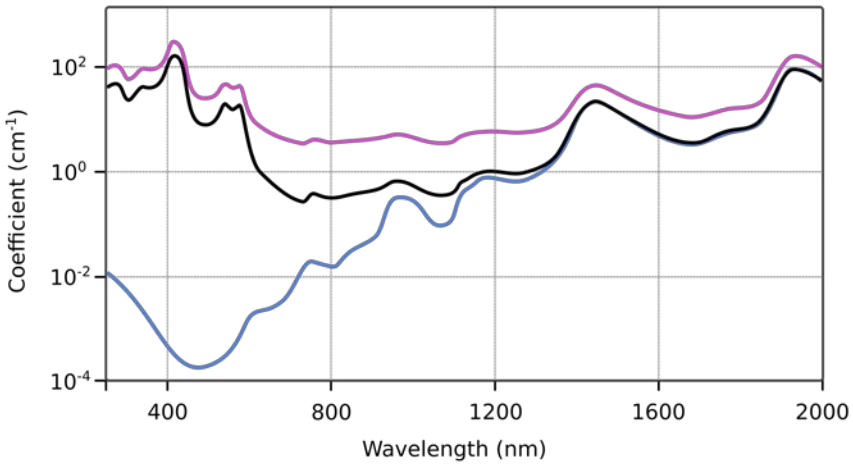

Figure 4. Sample vein absorption spectra, showing the absorption coefficient (black), effective absorption coefficient (magenta), and absorption for tissue containing 75% water (blue). Source[10].

The hyperspectral imager was therefore selected after the appropriate literature review and analysis of possible applications of the system to cover the NIR spectral range as fully as possible within the current technological limitations.

The rest of this paper contains a description of the proposed initial demonstrator system in the next chapter, followed by a brief comparison of the apparatus to related medical spectroscopy systems in Chapter 3. A summary of the results achieved so far is provided in Chapter 4.

2. SYSTEM DESCRIPTION

The architecture of the proposed system was designed to fulfill the primary use case, which is navigation during the (minimally) invasive laparoscopic or surgical operations. In an ideal case, the end user of the imaging system has high effective spatial, spectral, and temporal resolution at his or her disposal. Since this cannot be currently realized by a single image sensor, the described system uses a dual sensor configuration to achieve high effective resolution in all aforementioned areas[11].

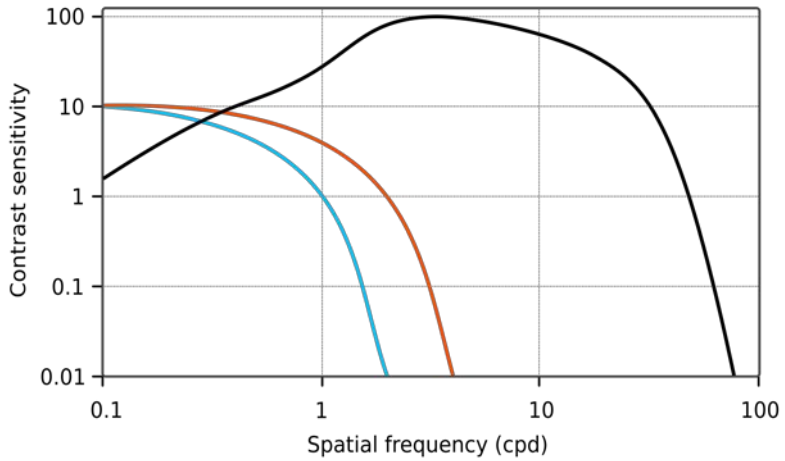

Figure 5. Spatial contrast sensitivity functions for luminance (black) and chromatic contrast (blue-yellow and red-green). Source[12].

The system was designed with regard to specific properties of the human vision system in mind. The human eye uses photosensitive cells to reconstruct the image present on the retina with rod cells being sensitive to (monochromatic) luminance and cone cells being sensitive to the three primaries red, green, and blue, together forming the trichromatic color vision system. As can be seen in Fig. 5, the spatial contrast sensitivity for luminance of the human eye is higher than its chromatic contrast sensitivity[12]. This can be restated as luminance component having a higher effective spatial resolution compared to the chromatic component. This principle is widely used in video distribution and compression standards, where the color components of the individual pixel representations are transferred with lower spatial resolutions (subsampled) compared to the luminance components with no significant impact on the perceived (effective) video quality[13]. An example image with the chromatic component spatially downsampled is given in Fig. 6.

Figure 6. Sample image demonstrating the chroma subsampling principle. Compared to the original image (left), an image with the chromatic component subsampled 10× in each dimension contains no significant chromatic artifacts (right).

Based on this characteristic of human vision, one of the ways of combining the image data is to use the luminance data from the sensor with high spatial resolution and merge it with the processed data from the high spectral resolution sensor as a chrominance (color) component of the combined video signal. The spectral data processing functions can be formed by any algorithm, provided its output maps into the human vision color space[5].

The concept of the proposed system is based on a standard medical endoscope camera system. The device consists of two main parts, camera head and a main digital signal processing unit, which are connected together using a flexible cable carrying data, control signals, and power to the camera head. The mechanical dimensions and power consumption of both subsystems is comparable to standard off-the-shelf medical camera systems.

The camera head was designed to mimic a regular of the shelf medical endoscope system. This was considered advantageous to the usability of the camera and general reception by the end users. The camera head utilizes a flexible cable connection and is compatible with a large set of endoscopic accessories.

Since the camera head and processing unit are only a part of a larger medical device ecosystem, the camera head features a C-mount lens thread to connect to a wide variety of off-the-shelf optical components to allow for an easy medical evaluation of the system. For endoscopic use, the system contains an endoscope to C-mount adaptor to connect to the endoscopic apparatus itself together with the supporting light source.

The mechanical enclosure of the camera head was designed using CAD/CAM software. It is manufactured from aluminum alloy and the surface is treated with black anodizing to minimize internal reflections and provide a durable enclosure. The mechanical design (as shown in Fig. 7) is rather basic, since the main purpose is currently a demonstration system.

The optical path of the camera head was designed to simultaneously sample the region of interest by the two image sensors, as illustrated in Fig. 8. Since the C-mount lens focuses the image onto a single image plane, the system contains a beam splitter to create the two required image planes, one image plane for the visible light sensor and one for the NIR hyperspectral image sensor[5]. To remove the unwanted wavelengths from the hyperspectral image sensor, a longpass and a shortpass optical filters are installed as required by the sensor manufacturer. Because of mechanical constraints, the shortpass filter is located in the optical path before the beam-splitter and is therefore common to both sensors. The longpass filter is located between the beam-splitter and the hyperspectral NIR imager. With this configuration, the spectral range of incoming radiation is correctly limited for the hyperspectral sensor and the visible light sensor is not

affected by this shared filter since it is outside of its spectral working range. Due to the number of components required in the optical path, it was not possible to maintain the required C-mount 17.526 mm flange focal distance. For this reason, an additional negative achromatic doublet was placed into the optical path before the beam-splitter to offset the focus plane further. Although this increased the effective focal distance of the optical system and in principle works as a teleconverter (Barlow lens), it was deemed acceptable since it allowed the system to focus to infinity, which was not possible with the initial optical configuration without the achromatic doublet.

Figure 7. Camera head prototype.

Being a prototype demonstrator, it was so far not possible to have all of the optical elements of the system optimized for the extended 400 nm - 1000 nm visible and NIR ranges (this concerns mainly the antireflection coatings) and therefore priority was given to the NIR range, where required. The system currently uses lens not optimized for the extended 400 nm - 1000 nm range and therefore the focusing works slightly differently for the sensors because of the different spectral ranges. For the time being, this is not considered a major issue and will be addressed in future versions of the system.

The image sensors are mounted using precision adjustable screws to fine-tune the position of the sensor with respect to its image focus planes. Any incorrect alignment other than the parallel alignment to the focus plane can be corrected digitally by standard image rotation, translation and scaling blocks during the subsequent signal processing stages.

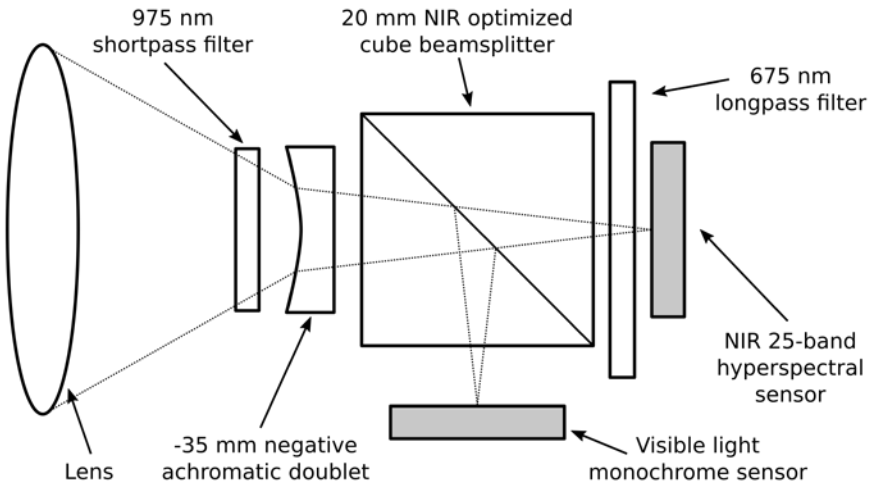

Figure 8. Camera head optical path configuration.

As described in previous sections, the sensors have different spatial and spectral resolutions. Since both imagers are built using a standard CMOS image sensor technology, the temporal resolution is the same and usable for real-time video acquisition. The hyperspectral NIR image sensor has a 25-band configuration with physical resolution of 2048 × 1088 pixels. The 25 bands are arranged in a 5 × 5 physical pixels grid and (with some clipping to a more standard video resolution) the effective resolution is 384 × 216 hyperspectral pixels (Full HD dimensions divided by 5). The visible light sensor is a monochrome sensor with the same physical resolution, therefore the visible light image has a resolution of 1920 × 1080 (again after some clipping).

In place of the image sensor with high spatial resolution can be either a standard monochrome or color (RGB) sensor, since even a three-band color sensor has a significantly higher spatial resolution compared to any hyperspectral image sensor with the same physical pixel resolution due to the higher number of spectral bands[5]. The advantage of the monochrome sensor lies in its higher effective spatial resolution compared to the color image sensor. The advantage of the RGB sensor is that it can deliver standard visible light true color image, while still providing relatively high spatial resolution. An useful usage scenario of the system might be the simultaneous display of the monochrome (or color) visible light image together with the processed and combined false color image (for example in the side by side screen layout) merged into the system video output signal.

Since the device will be used for hand-eye coordination during medical procedures, a very low system latency is critical. This is achievable rather easily due to the fact that both sensors are classical CMOS imagers and are therefore capable of frame rates well above the industry standard of 60 Hz. This high temporal resolution requirement also places a hard real-time constraint on the maximum time available for spectral data processing algorithms to perform the analysis of one video frame. When configured for a standard video refresh rate of 60 Hz, the frame time is approximately 17 ms.

The system electronics is split between the camera head and a main processing unit. The main element of both subsystems is a field programmable gate array (FPGA). The camera head uses a relatively small FPGA to receive the raw data from the image sensors, perform basic data reprocessing, and repack the data stream into a form suitable for transmission over a high-speed serial interface through a flexible cable to the main system unit. A top-level overview of the signal processing is given in Fig. 9.

The main unit circuit board contains an FPGA for the implementation of visible light and hyperspectral image data processing algorithms and the subsequent image fusion of luma and chroma components to form the resulting image[5]. The image data are represented using the RGB color space during the processing stages. For the merge operation, the video streams are converted to the YCbCr color space, widely used in video distribution and compression systems. After the conversion, the streams are merged together, converted back to the RGB color space and sent to the video output of the system for display on a monitor. The main processing board can be also used for the optional translation, rotation and scaling of the two video streams to achieve a good image alignment of the individual video frames.

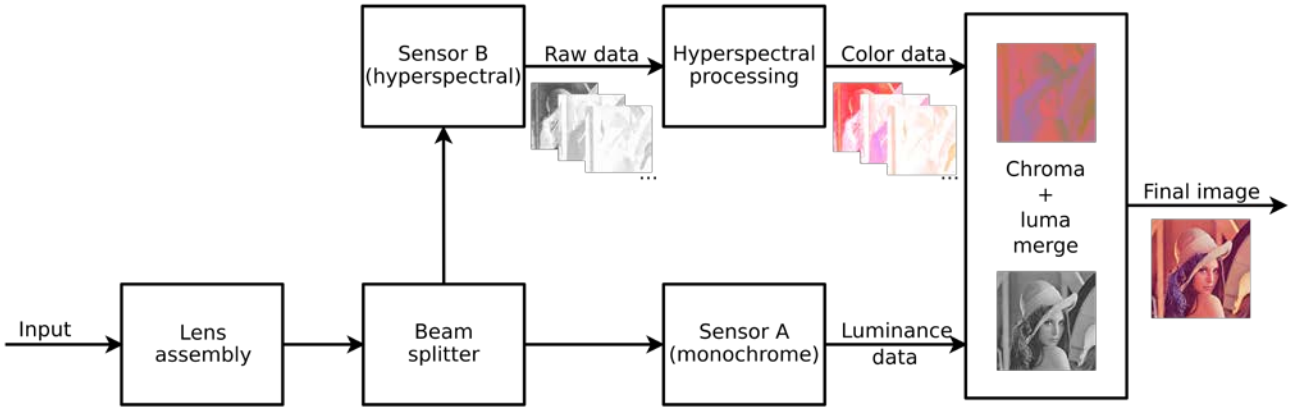

Figure 9. Block diagram of video data processing and merging of the proposed system.

The current preliminary instantiation of the demonstrator comes with a rather basic functionality, such as spectral band selection, where a selected spectral band is converted using a color map stored in a lookup table and displayed on the system video output. This basic implementation could be (in principle) used e.g. for fluorescence imaging, where the required band can be selected by the user depending on the fluorescence marker that is used in the experiments.

The next step for the system development is the implementation of a suitable, computationally efficient algorithm for spectral similarity ranking. A suitable candidate algorithm is the normalized Euclidean distance (NED), for example, which can be implemented relatively easily in hardware and its performance is comparable or better than the commonly used spectral angle or spectral correlation angle algorithm[14]. The implementation of the NED algorithm does not introduce any significant latency to the video processing path and therefore is suitable for real-time applications of the proposed device.

3. COMPARISON TO OTHER SYSTEMS

In spectral imaging applications, some tradeoff between spatial, spectral, and temporal resolution must usually be made. The main time consuming tasks of spectral imaging systems are image acquisition and data processing. High spectral or spatial resolution requires more processing time, which results in low temporal resolution.

To the best of our knowledge, currently available medical spectroscopy systems have limited capabilities when considering real-time applications. Specifically, the hand-eye coordination functionality required during the invasive or minimally invasive laparoscopic procedures is in most cases missing. An overview of selected medical spectroscopy systems is provided in Table 1.

To overcome these limitations, many systems use two detectors, one for spectral imaging and the other for visible light. For example, a preliminary demonstrator of burn wound healing time estimation device uses three bands - red, green, and infrared. The video camera captures the light through color filter wheel that is synchronized to the 60 Hz camera frame rate. The device is capable of processing the data in 30 seconds[15].

Systems designed to perform a specific function, such as fluorescent dye tracking, have low spectral resolution (2 or 3 NIR bands) and contain a visible light image sensor for navigation[16]. The authors developed a system using commercial surgical microscopy and a near infrared laser. The maximum frame rate for fluorescence imaging is approximately 45 frames per second, but this number is decreased when a clear image with better signal to noise ratio is needed. A related imaging system is FLARE™, able to acquire color video (400 – 650 nm visible light) images simultaneously with NIR fluorescence images (2 bands), at frame rates up to 15 Hz[17,18]. Other commercial multispectral microscopy systems produce a video stream of one NIR band[19] or combine one NIR band with one or more visible light bands[20].

In comparison, the system described in this article has the capability to (in principle) perform same functions as the aforementioned devices, since the user can select a spectral band of interest from the hyperspectral image sensor. The

current version of the demonstrator contains hyperspectral sensor with 25 bands covering mostly the lower NIR wavelength range. All wavelength bands, including the visible light color or monochrome images, can be processed and displayed simultaneously with a refresh rate of 60 Hz or more.

Another class of spectroscopy systems uses multi-spectral imaging to capture spectral profiles of the region of interest. Different technologies are employed to acquire the high spectral resolution images. For example, in[11], the authors propose a system for near real-time imaging at 3 frames per second. The device utilizes a digital light processing (DLP) technology to illuminate the region of interest with predetermined spectra. The light originating from a light source is focused onto a dispersion grating and illuminates the various comprising spectral bands onto successive columns of the micromirror array. To create the desired spectral illumination, the intensity of each spectral bandpass is controlled by triggering the appropriate number of micromirrors. For each wavelength-dependent column, the micromirrors reflect the light either to a heat sink or to the beam shaping optics that illuminates the target ROI. However, the system has serious drawbacks that limit its utility in operating room, since (for example) all lights must be turned off during the image acquisition phase. In addition, stable measurements can be taken by the apparatus only after approximately 35 minutes of the initial warm-up phase.

In comparison, the hyperspectral sensor of the proposed system has filters located directly atop of the physical CMOS pixels, therefore the sensor will generate a suitable response for all wavelengths within the sensor spectral working range.

Spectroscopy systems using the Fourier transform infrared (FTIR) method for spectral image acquisition feature high spectral and optionally a high spatial resolution as well. The downside however, is the acquisition time for a single image. For example, the FTIR spectrometer proposed in[21] acquires 4096 bands for every single FTIR image, with each spectrum being the average of 256 scans recorded in about 5 minutes.

Another type of spectroscopy system is based on liquid crystal tunable filter (LCTF) technology coupled to an endoscope[22]. The LCTF based device is capable of capturing images with a large number of bands (10 – 100) with very narrow spectral widths of the individual bands. The system uses an ICCD camera with a 5 frames per second output. Each image has a resolution of approximately 150 pixels along the diameter of the fiber optics bundle. The total acquisition time for the full spectral image is 23 seconds, therefore the authors manually selected five bands in order to reduce the acquisition time to approximately 1 second.

The imaging system proposed in this article does not have a very high spectral resolution, on the other hand the 25 spectral bands allow to implement a number of useful applications. However, the spatial resolution (in combination with the visible light sensor) and temporal resolution remain relatively high.

Table 1. A comparison of main parameters of related medical spectroscopy imaging systems.

	Spectral range	Spatial resolution (pixels)	Spectral resolution (bands)	Temporal resolution (Hz)	Enhanced and color video
Burn estimator device[15]	Red, Green , 880nm NIR	480 x 512	2 color bands + 1 NIR band	0.033	False-color images
FLARE[18]	VIS, 700nm and 800nm NIR	640 x 480 (three sensors)	3 bands + 3 color bands	15	Yes
SPY Elite[19]	800 NIR	752 x 480	1 band	30	No
Leica FL800 / DFC7000T camera[20]	VIS, 820nm NIR	1024 x 768	1 band + 3 color bands	40	Yes
Active DLP[11]	380 to 780 nm	1392 x 1040	126 bands	0.33	No
Hyperion 3000 FTIR[21]	5882-6250	~	Up to 4096 bands	0.0033	No
LCTF system[22]	420–700 nm	150	5 bands	1	No
Proposed system	VIS, 600-1000 NIR	384 x 216 NIR, 1920 x 1080 VIS	25 bands + 3 color bands	60, up to 340 (not impl.)	Yes

4. CONCLUSION

In this paper, a demonstrator system was proposed which tries to compensate for the limited spatial, spectral and temporal resolutions of the currently available image sensors. The dual sensor configuration is relatively easy to implement and coupled with the subsequent digital signal processing this setup allows for a vast improvement of the useful information present in the video output of the system. The fact that the system uses in principle standard CMOS image sensors allows it to operate at high enough frame rates and low enough latency to be usable as a standard video source, therefore enabling hand-eye coordination functionality.

Although being an initial demonstrator apparatus, the system is being continuously developed and in time will be used in real world medical settings. The selected lower end of the NIR spectrum includes a range of interesting biophysical properties, beyond the tissue differentiation, interesting detectable features include for example hemoglobin oxygenation levels, which could enable the visualization of oxygenated and deoxygenated blood in real time during medical surgeries. Some subsurface imaging functionality may also be a viable path due to the NIR optical window being present in the system spectral sensitivity range.

An advantage of the proposed system is the small physical size. The camera head measures approximately 50 mm × 50 mm × 70 mm, this is comparable to standard off-the-shelf medical endoscope systems. A further device miniaturization is possible with a more advanced mechanical design of the camera head.

The demonstrator uses an FPGA as the main digital signal processing element, this provides a way to implement the processing algorithms on a very low level with minimal latency together with the flexibility to swap and modify the signal processing modules.

ACKNOWLEDGEMENTS

This work is funded in part by the Technology Agency of the Czech Republic (TA CR) under grant agreement TA04010776 Research and development of innovative imaging system for more accurate image based navigation during invasive surgeries using hyperspectral imaging. The project is also funded by IBSmm Engineering spol. s r.o. from nonpublic sources.

REFERENCES

[1] Lu, G.., Fei, B., “Medical hyperspectral imaging: a review,” Journal of Biomedical Optics 19(1), 10901 (2014).

[2] Koshikawa, Y.., Machida, R., “Light source apparatus and endoscope system,” US20120130175 A1 (2012).

[3] Geelen, B., Tack, N.., Lambrechts, A., “A compact snapshot multispectral imager with a monolithically integrated per-pixel filter mosaic,” 7 March 2014.

[4] Bayer, B. E., "Color imaging array", US 3971065 A (1976).

[5] Roth, F., “Hyperspectral imaging system for medical dermatology or endoscopy, method of scanning by the hyperspectral imaging system and use thereof,” CZ 306066 B6 (2016).

[6] Murkin, J. M.., Arango, M., “Near-infrared spectroscopy as an index of brain and tissue oxygenation,” British Journal of Anaesthesia 103(Supplement 1), i3–i13 (2009).

[7] Matcher, S. J., Cope, M.., Delpy, D. T., “Use of the water absorption spectrum to quantify tissue chromophore concentration changes in near-infrared spectroscopy,” Physics in Medicine and Biology 39(1), 177–196 (1994).

[8] Sakudo, A., Kato, Y. H., Tajima, S., Kuratsune, H.., Ikuta, K., “Visible and near-infrared spectral changes in the thumb of patients with chronic fatigue syndrome,” Clinica Chimica Acta 403(1–2), 163–166 (2009).

[9] Zuzak, K. J., Naik, S. C., Alexandrakis, G., Hawkins, D., Behbehani, K.., Livingston, E., “Intraoperative bile duct visualization using near-infrared hyperspectral video imaging,” The American Journal of Surgery 195(4), 491–497 (2008).

[10] “Near-infrared window in biological tissue - Wikipedia, the free encyclopedia.”, <https://en.wikipedia.org/wiki/Near-infrared_window_in_biological_tissue#/media/File:Veins_absorption.png> (9 September 2016).

[11] Zuzak, K. J., Francis, R. P., Wehner, E. F., Litorja, M., Cadeddu, J. A.., Livingston, E. H., “Active DLP Hyperspectral Illumination: A Noninvasive, in Vivo, System Characterization Visualizing Tissue Oxygenation at Near Video Rates,” Analytical Chemistry 83(19), 7424–7430 (2011).

[12] Fairchild, M. D., Color appearance models, 2nd ed, J. Wiley, Chichester, West Sussex, England ; Hoboken, NJ (2005).

[13] Branden Lambrecht, C. J. van den, ed., Vision models and applications to image and video processing, Kluwer Academic, Boston (2001).

[14] Robila, S. A.., Gershman, A., “Spectral matching accuracy in processing hyperspectral data,” 2005, 163–166, IEEE.

[15] Afromowitz, M. A., Callis, J. B., Heimbach, D. M., DeSoto, L. A.., Norton, M. K., “Multispectral imaging of burn wounds: a new clinical instrument for evaluating burn depth,” Biomedical Engineering, IEEE Transactions on 35(10), 842–850 (1988).

[16] Lee, C., Lee, D., Zhou, Q., Kim, J.., Kim, C., “Real-time Near-infrared Virtual Intraoperative Surgical Photoacoustic Microscopy,” Photoacoustics 3(3), 100–106 (2015).

[17] Matsui, A., Tanaka, E., Choi, H. S., Kianzad, V., Gioux, S., Lomnes, S. J.., Frangioni, J. V., “Real-time, near-infrared, fluorescence-guided identification of the ureters using methylene blue,” Surgery 148(1), 78–86 (2010).

[18] Troyan, S. L., Kianzad, V., Gibbs-Strauss, S. L., Gioux, S., Matsui, A., Oketokoun, R., Ngo, L., Khamene, A., Azar, F., et al., “The FLARE^{TM} Intraoperative Near-Infrared Fluorescence Imaging System: A First-in-Human Clinical Trial in Breast Cancer Sentinel Lymph Node Mapping,” Annals of Surgical Oncology 16(10), 2943–2952 (2009).

[19] Docherty, J. C., Hewko, M., Mangat, G., Flower, R. W.., Chari, S. M., “Method and apparatus for performing intra-operative angiography,” US 8,892,190 B2.

[20] “Leica FL800 - Product: Leica Microsystems.”, <http://www.leica-microsystems.com/products/surgical-microscopes/neurosurgery-spine/details/product/leica-fl800/> (27 July 2016).

[21] Kumar, S., Desmedt, C., Larsimont, D., Sotiriou, C.., Goormaghtigh, E., “Change in the microenvironment of breast cancer studied by FTIR imaging,” The Analyst 138(14), 4058 (2013).

[22] Martin, M. E., Wabuyele, M. B., Chen, K., Kasili, P., Panjehpour, M., Phan, M., Overholt, B., Cunningham, G., Wilson, D., et al., “Development of an Advanced Hyperspectral Imaging (HSI) System with Applications for Cancer Detection,” Annals of Biomedical Engineering 34(6), 1061–1068 (2006).